

# Ring-Opening Polymerization of Lactones and Lactides with Sn(IV) and Al(III) Initiators

Henrik von Schenck,<sup>†</sup> Maria Ryner,<sup>‡</sup> Ann-Christine Albertsson,<sup>\*,‡</sup> and Mats Svensson<sup>\*,§</sup>

Materials Physics, Royal Institute of Technology, SE-100 44 Stockholm, Sweden; Department of Polymer Technology, Royal Institute of Technology, SE-100 44 Stockholm, Sweden; and Department of Chemistry, Organic Chemistry, Royal Institute of Technology, SE-100 44 Stockholm, Sweden

Received September 20, 2001

**ABSTRACT:** A theoretical study is presented of the ring-opening polymerization (ROP) mechanism of 1,5-dioxepan-2-one (DXO) and glycolide with Sn(II) and Al(III) alkoxide initiators (SnMe<sub>3</sub>MeO, SnMe<sub>2</sub>(MeO)<sub>2</sub>, and AlMe<sub>2</sub>MeO). The B3LYP density functional method has been used to perform the quantum chemical calculations. A coordination–insertion mechanism is presented with two principal reaction steps. First, the alkoxide of the initiator performs a nucleophilic attack on the carbonyl carbon, and the carbonyl bond is broken. An intermediate is formed at this point, where the former carbonyl oxygen of the monomer is coordinated to tin via an alkoxide bond, while the carbonyl carbon assumes a sp<sup>3</sup> bonding geometry. The second step involves the acyl–oxygen cleavage of the monomer. For all three initiators it was found that the transition state involving the breaking of the carbonyl double bond (**TS1**) represented the highest point on the potential energy surface for DXO. For glycolide, however, the transition state of the acyl–oxygen cleavage (**TS2**) was the least stable structure. The reaction barriers were calculated to 17.1 kcal/mol for DXO/SnMe<sub>3</sub>MeO, 18.7 kcal/mol for glycolide/SnMe<sub>3</sub>MeO, 14.3 kcal/mol for DXO/SnMe<sub>2</sub>(MeO)<sub>2</sub>, 14.5 kcal/mol for glycolide/SnMe<sub>2</sub>(MeO)<sub>2</sub>, 13.6 kcal/mol for DXO/AlMe<sub>2</sub>MeO, and 9.3 kcal/mol for glycolide/AlMe<sub>2</sub>MeO. Both electronic and steric properties of the monomer affect the reaction barriers. It was found that the more electrophilic initiators polymerized cyclic esters faster.

## Introduction

The majority of resorbable polymers used in the field of implant materials are synthesized by ring-opening polymerization (ROP) of cyclic esters. Aliphatic polyesters have successfully been modified in different ways, and the field of applications is ranging from resorbable sutures to controlled drug release systems. New polymers are continuously being synthesized, and there is still a great demand for new materials and for improved synthetic pathways. It is therefore important to gain a fundamental understanding of the mechanistic factors controlling the synthesis.

The most widely used initiators for ROP of cyclic esters are various tin and aluminum alkoxides. These initiators' predominance is due to their ability to produce stereoregular polymers<sup>1–5</sup> of narrow molecular weight distribution and controllable molecular weight,<sup>6–9</sup> with well-defined end groups.<sup>10</sup> The polymerization mechanism has been investigated for many years, and the coordination–insertion mechanism proceeding via acyl–oxygen cleavage of the monomer with insertion into the metal–oxygen bond of the initiator has been established. The most commonly used tin initiator is stannous(II) ethylhexanoate (SnOct<sub>2</sub>). There has been some controversy regarding the ROP mechanism of this initiator, but the coordination–insertion mechanism is now accepted, and the initiating species has been proven to be a tin alkoxide, formed prior to polymerization.<sup>11–15</sup>

A major difference between tin- and aluminum-based initiators is that tin initiators are good transesterification catalysts whereas aluminum initiators are not. This

makes the aluminum-based initiators more favorable for the synthesis of advanced macromolecular structures, since their polymerizations are more controllable. Extensive experimental investigations of different aluminum initiators have been performed by a number of groups.<sup>16–19</sup>

Tin initiators have the advantage of being more hydrolytically stable than their aluminum counterparts and are hence easier to handle and to use in polymerizations. After several years of research on tin alkoxides, controlled polymerizations of advanced structures are now possible. Under mild reaction conditions the undesirable transesterification reactions are less pronounced, and structures like triblocks,<sup>20</sup> macrocyclics,<sup>21</sup> multiblocks,<sup>22</sup> resorbable networks,<sup>23</sup> and star-shaped structures<sup>24</sup> can be prepared.

To summarize, research of the ROP of cyclic esters is a very active and expansive field. The work thus far has mainly been focused on the synthesis of new tin and aluminum initiators, with the goal of increasing reactivity and producing novel polymer structures. The aim of this paper has been to study the reaction mechanism of tin and aluminum alkoxides initiating polymerization of cyclic esters, trying to uncover what factors govern the reactivity of these systems. To achieve this, we used a quantum chemical approach, a valuable method for studying reaction mechanisms that are hard to investigate by kinetic studies, spectroscopic, or chromatographic methods.<sup>11,19,25</sup> Comparisons are made between different monomers and different initiators and between experimental and theoretical results.

## Computational Details

Geometries and energies of all intermediates were optimized using the gradient-corrected density func-

<sup>†</sup> Materials Physics.

<sup>‡</sup> Department of Polymer Technology.

<sup>§</sup> Department of Chemistry, Organic Chemistry.

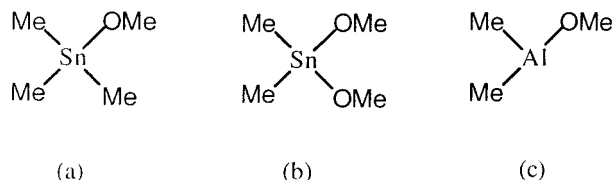


**Figure 1.** Structures of the investigated ROP initiators: (a)  $\text{SnMe}_3\text{MeO}$ , (b)  $\text{SnMe}_2(\text{MeO})_2$ , and (c)  $\text{AlMe}_2\text{MeO}$ .

**Table 1. Overview of the Investigated Sn(IV) and Al(III) Systems**

system	initiator	monomer
A	$\text{SnMe}_3\text{MeO}$	DXO
B	$\text{SnMe}_3\text{MeO}$	GA
C	$\text{SnMe}_2(\text{MeO})_2$	DXO
D	$\text{SnMe}_2(\text{MeO})_2$	GA
E	$\text{AlMe}_2\text{MeO}$	DXO
F	$\text{AlMe}_2\text{MeO}$	GA

tional method B3LYP.<sup>26</sup> This popular and computationally relatively cheap method has been shown to predict reliable geometries and energies.<sup>25,27–36</sup> A basis set of double- $\zeta$  valence quality labeled LANL2DZ was used in the Gaussian98 program.<sup>37</sup> A relativistic electron core potential (ECP) developed by Hay and Wadt replaced the tin core electrons.<sup>38,39</sup> For nonmetal atoms the double- $\zeta$  basis sets of Huzinaga and Dunning were assigned.<sup>40,41</sup> We recalculated all energies using a triple- $\zeta$  contracted basis set at the B3LYP level, i.e., the 6-311G(d,p) basis set,<sup>42,43</sup> for all non metal atoms and a 3s3p contraction of the Hay and Wadt primitive basis set for tin and aluminum augmented with one d-function (0.18 and 0.19, respectively). The character of all intermediates and transition states was checked by performing frequency calculations.

## Results and Discussion

We have studied the ROP mechanism of DXO and glycolide with three different initiators. The model initiators  $\text{SnMe}_3\text{MeO}$ ,  $\text{SnMe}_2(\text{MeO})_2$ , and  $\text{AlMe}_2\text{MeO}$  (Figure 1) were chosen since they resemble some of the most investigated tin and aluminum initiators.

DXO and glycolide were chosen as model monomers. Experimental data of the ROP of DXO with different tin and aluminum initiators have been gathered by Albertsson et al.<sup>6,9</sup> Glycolide was chosen to represent the central structural and electronic features of lactide, relevant to the ROP mechanism.

The systems investigated are summarized in Table 1. The optimized structures during ring-opening polymerization of the  $\text{SnMe}_3\text{MeO}$ /DXO system (A) are presented in Figures 2 and 3. Intermediates and transition states **1–4** for systems B–F are analogous to the structures in Figures 2 and 3. Significant differences between the systems will be commented upon with reference to system A (DXO/ $\text{SnMe}_3\text{MeO}$ ).

**The ROP Mechanism.** The first part of the initiation/propagation involved the coordination of the monomer to the initiator species **1a**, forming the precursor structure **2a** (Figures 2 and 3). With the coordination of the monomer, the alkoxy group performed a nucleophilic attack at the monomer's carbonyl carbon. The formation of the new C–O bond between the monomer and the alkoxy group occurred via the four-center transition state **TS1a**. In intermediate **3a**, the former carbonyl oxygen was coordinated to tin via an alkoxide

bond, while the carbonyl carbon assumed a  $\text{sp}^3$  bonding geometry. This arrangement allowed for rotation around the C–O axis, enabling the acyl oxygen in the ring to rotate into position for the ring-opening step. For DXO the activation energy for the acyl–oxygen cleavage, 8.3 kcal/mol, was notably lower than the barrier for breaking the carbonyl bond and forming a new C–O bond, 17.1 kcal/mol. The initiation/propagation was completed with the formation of **4a**, the analogue to species **1a**.

The relative energies of all investigated structures of systems A–F are given in Table 2, along with the potential energy surfaces, represented in Figure 4.

From the potential energy surfaces presented in Figure 4, some very interesting trends can be noted. Perhaps the most striking observation is that the rate-determining step of the ROP was different for the two monomers. Breaking the carbonyl double bond and forming a new C–O bond (**TS1**) represented the highest point on the potential energy surface, in the case of DXO. For glycolide, however, the transition state of the acyl–oxygen cleavage (**TS2**) was the least stable structure. This can be explained by a closer inspection of the monomer properties. The carbonyl double bond in the monomer must be broken in order to form the intermediate structure **3**. The energy required to break such a bond was found to be 4.2 kcal/mol lower for glycolide.<sup>44</sup> This explains why the reaction barrier of (**2-TS1**) is higher for DXO. As for the acyl–oxygen cleavage of the monomer, the difference in barrier height (**3-TS2**) between DXO and glycolide with the same initiator can tentatively be explained by the ability to accommodate the induced ring strain in **TS2**. The six-membered glycolide ring is inherently more rigid since it contains two carboxyl components of  $\text{sp}^2$  character.

For the tin initiators  $\text{SnMe}_3\text{MeO}$  and  $\text{SnMe}_2(\text{MeO})_2$ , we found that DXO should undergo ROP somewhat faster than glycolide. In the case of  $\text{AlMe}_2\text{MeO}$ , however, calculated values suggested that DXO should polymerize much slower than glycolide. The activation energies for ROP of the corresponding systems were 17.1 kcal/mol for system A, 18.7 kcal/mol for system B, 14.3 kcal/mol for system C, and 14.5 kcal/mol for system D. The difference was more pronounced for the  $\text{AlMe}_2\text{MeO}$  catalyst: 13.6 kcal/mol for system E and 9.3 kcal/mol for system F.

It has been found experimentally that DXO propagates faster than LL-lactide with  $\text{SnBu}_2(\text{MeO})_2$  and similar initiators.<sup>6,7,45</sup> The activation energy for DXO with  $\text{SnBu}_2(\text{MeO})_2$  has been estimated to be 17.0 kcal/mol.<sup>6</sup> The same initiator reacted approximately 10 times slower with LL-lactide under the same reaction conditions.<sup>7</sup> Furthermore, experiments have shown that  $\text{SnBu}_2(\text{EtO})_2$  polymerizes LL-lactide faster than  $\text{SnBu}_3\text{EtO}$ .<sup>46,47</sup> The results presented here for systems A–D agree well with the experimental data, and it appears that glycolide serves well as a model of lactides. However, the results obtained for system F (glycolide/ $\text{AlMe}_2\text{MeO}$ ) do not account for the experimental observations for similar systems. The absolute rate constant ( $k_{\text{abs}}$ ) for DL-lactide polymerization in toluene, 70 °C, with  $\text{AlEt}_2\text{OC}_2\text{H}_4\text{Br}$  is  $0.011 \text{ L mol}^{-1} \text{ min}^{-1}$ , compared to  $k_{\text{abs}} = 0.224 \text{ L mol}^{-1} \text{ min}^{-1}$  for ROP of DXO under identical reaction conditions.<sup>18,48,49</sup> The rate of polymerization of LL-lactide in THF, 80 °C, with  $\text{AlEt}_2\text{EtO}$  is also comparatively slow.<sup>46</sup>

To investigate the effect of the methyl substituents on lactide, we calculated the activation barrier for the

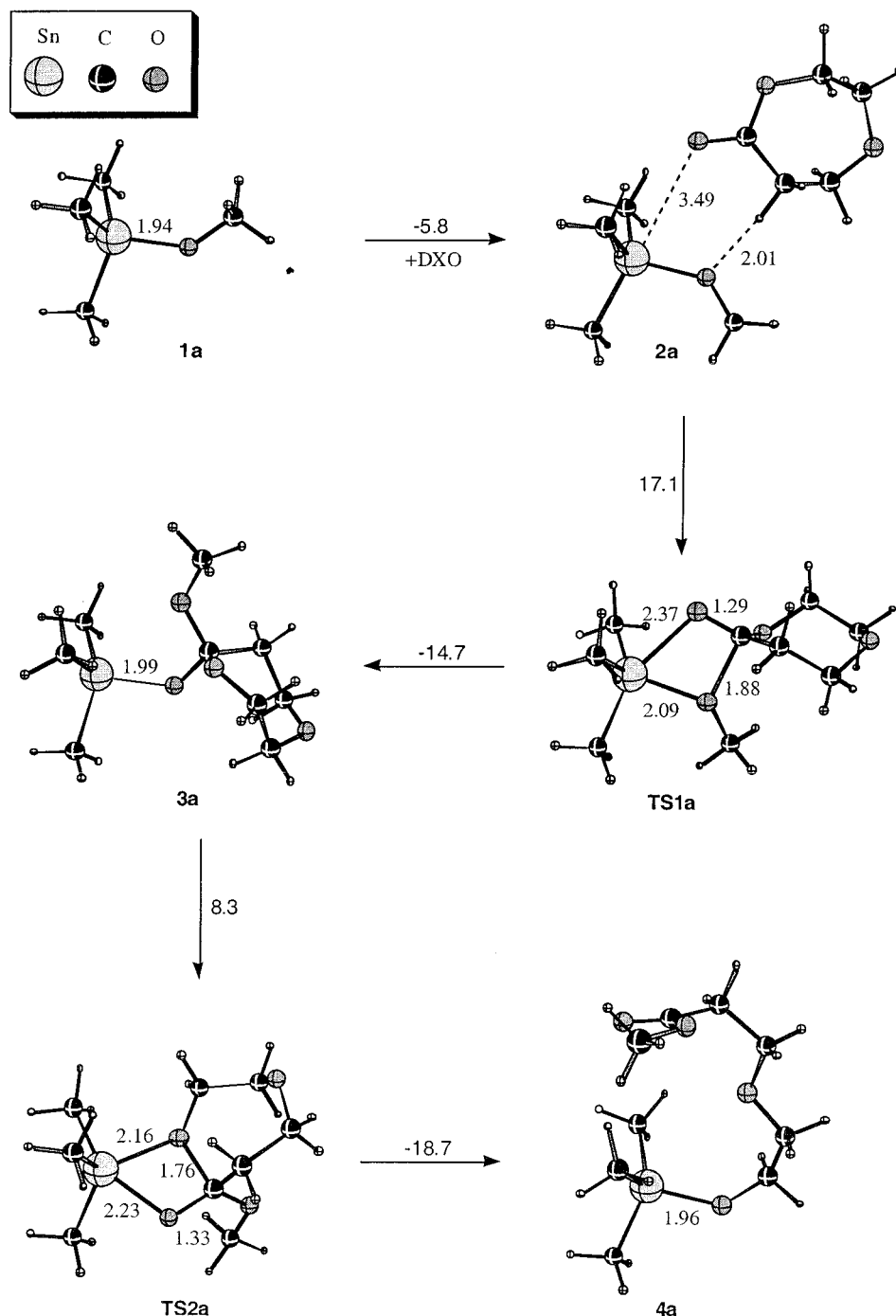


**Figure 2.** Structures of the intermediates and transition states involved in the ROP of DXO with  $\text{SnMe}_3\text{MeO}$  (system A). Distances are given in Å and energies in kcal/mol.

ROP of DL-lactide with both an Al(III) and a Sn(IV) initiator. A system F' was studied where DL-lactide was polymerized using  $\text{AlMe}_2\text{MeO}$ . This resulted in an activation energy of 13.1 kcal/mol, i.e., a barrier increase<sup>50</sup> by 3.8 kcal/mol compared to system F. We also calculated the reaction barrier for a system B' (DL-lactide/ $\text{Sn Me}_3\text{MeO}$ ) comparing the results to system B. We found the reaction barrier to be 19.3 kcal/mol for the DL-lactide monomer, i.e., a small increase<sup>51</sup> of 0.6 kcal/mol compared to system B. Clearly, the reaction barrier of the Al(III) initiator was significantly affected by the steric bulk of the methyl groups on the monomer ring, while it was essentially unaffected for the Sn(IV) initiator. A closer inspection of the transition states shows that steric interactions cause strain to be induced

into the structures in the case of DL-lactide. Figure 5 shows the structures of **TS2f** and **TS2f'**.

In the case of **TS2f'**, the steric interaction between methyl groups on the monomer and the initiator primarily lead to a shift in the position of C1, relative to **TS2f**. As an indicator of the ring distortion, it was found the dihedral angle  $\text{Al}-\text{O1}-\text{C1}-\text{C2}$  increased by  $43^\circ$ . In the corresponding transition-state structures for  $\text{SnMe}_3\text{OMe}$ , **TS2b** and **TS2b'**, the steric interactions caused considerably smaller alterations in the ring. The change in the dihedral angles ( $\text{Sn}-\text{O1}-\text{C1}-\text{C2}$ ) was  $15^\circ$ . The methyl groups on DL-lactide do not induce ring strain in the structures **2b'** or **2f'**.

It seems likely that the influence of monomer bulkiness on the potential energy surface can be related to

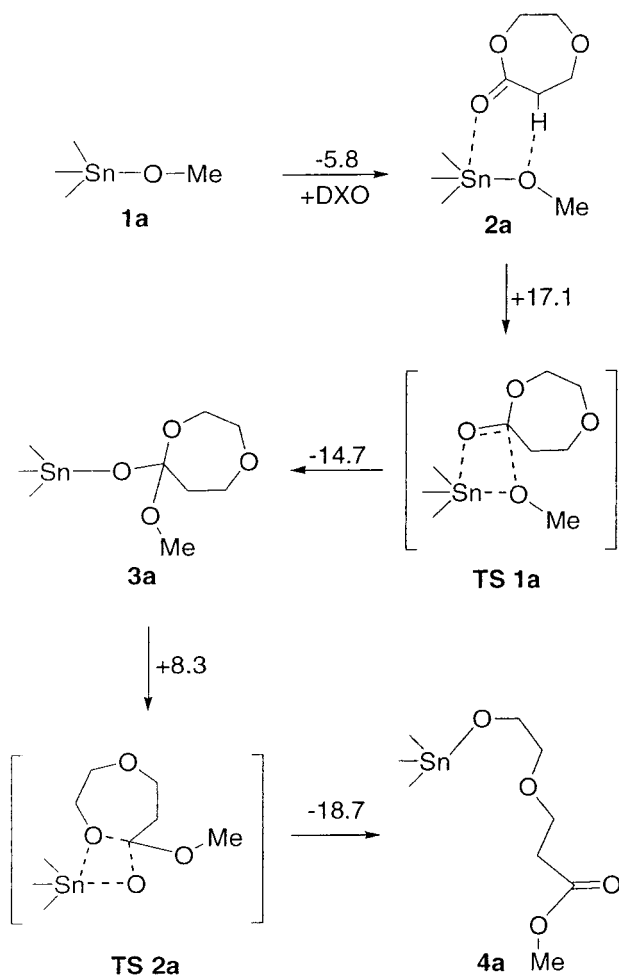


**Figure 3.** Schematic 2D representation of the reaction mechanism for the ROP of DXO with SnMe<sub>3</sub>MeO (system A). Energies are given in kcal/mol.

**Table 2. Relative Energies (kcal/mol) of the Intermediates and Transition States in the Ring-Opening Polymerizations of Systems A–F**

structure	A	B	C	D	E	F
<b>1</b>	5.8	6.7	11.5	10.4	21.2	18.4
<b>2</b>	0.0	0.0	0.0	0.0	0.0	0.0
<b>TS1</b>	17.1	12.7	14.3	7.8	13.6	6.9
<b>3</b>	2.3	-1.6	4.2	-1.3	6.6	5.1
<b>TS2</b>	10.6	17.1	9.1	13.2	7.1	9.3
<b>4</b>	-8.1	-13.4	-7.1	-12.8	-4.5	-15.0

the strength of the oxygen–metal bonds. The Al initiator, being more electronegative, displays shorter metal to oxygen bonds, in the range of 0.1–0.3 Å, compared to the corresponding structures of the Sn initiators. Therefore, it is no surprise that destabilization of structures along the potential energy surface is greater for Al, with an increasing bulk of the monomer. It can also be expected that sterically demanding ligands on the initiator can have similar effects.

It is interesting to note the influence of sterics of the reaction barriers of Sn and Al initiators. Below, it is concluded that initiators with a more electrophilic metal center tend to be more reactive for the studied monomers. It seems, however, that such initiators are also more sensitive with respect to steric interactions influencing the reaction barrier. This may have intriguing effects on the design of future initiator/monomer systems. An extensive investigation of steric influences on the reactivity in ROP with strongly electrophilic initia-

tors is currently under way in our group. Preliminary results show that the character of the potential energy surface does not change for the system DL-lactide/AlMe<sub>2</sub>MeO compared to glycolide/AlMe<sub>2</sub>MeO; i.e., the relative stabilities of the structures **1–4** are the same.

**Comparison of Initiators.** The electrophilicity of the metal center plays an important role in the ROP reaction sequence. The propensity toward metal–oxygen bond formation followed the accessibility of the initiator's lowest unoccupied molecular orbital (LUMO). The energy of the LUMO was 6.5 kcal/mol higher for SnMe<sub>3</sub>MeO compared to that of SnMe<sub>2</sub>(MeO)<sub>2</sub>, which in turn was 4.0 kcal/mol higher than that of AlMe<sub>2</sub>MeO.<sup>52</sup> Several trends correlate with the relative differences between the energy levels. First of all, we noted that the monomer coordination strength followed the sequence SnMe<sub>3</sub>MeO < SnMe<sub>2</sub>(MeO)<sub>2</sub> < AlMe<sub>2</sub>MeO. A stronger coordination of the monomer to the metal will lead to an increased polarization of the active carbonyl. This should in turn translate into a lower barrier of activation for the steps **2–TS1–3**. As can be seen from the potential energy surfaces in Figure 4, we found that the barrier decreased in the following order: SnMe<sub>3</sub>MeO > SnMe<sub>2</sub>(MeO)<sub>2</sub> > AlMe<sub>2</sub>MeO. The activation barrier of the acyl–oxygen cleavage, **3–TS2–4**, followed the same trend, which can be explained by similar arguments. First, we note the close relation between the intermediate **3** and the free initiator **1**. For instance, in the case of system A **1a** and **3a** both have the character of SnMe<sub>3</sub>RO; i.e., the metal center will have similar electronic properties in both structures. Second, the formation of **TS2** involves a bond being created between the endocyclic oxygen and the initiator metal. The donation of the oxygen lone pair to the metal is facilitated by a stable unoccupied molecular orbital; i.e., the initiator with the lowest lying LUMO will have the lowest **TS2**. The stability of the initiator LUMO correlated with the overall driving force of the reaction. For instance, in the case of DXO the energy difference between structures **1** and **4** is -13.9 kcal/mol for system A, -18.6 kcal/mol for system C, and -25.7 kcal/mol for system E. An increasing thermodynamic driving force tends to decrease the relative energy of the associated transition state. This is what is observed for both **TS1** and **TS2**. Experimental results agree with the general trend that more electrophilic initiators polymerize cyclic esters more rapidly.<sup>6,7,9,17,18,48</sup>

**Comparison of Sn(IV) and Sn(II) Initiators.** We have previously investigated the reaction mechanism of the ROP of DXO and LL-lactide with stannous(II) ethylhexanoate (SnOct<sub>2</sub>), using quantum chemical calculations.<sup>11</sup> In this case Sn(II) acetate (SnOct'<sub>2</sub>) and methanol were used as a model of the initiating complex. The SnOct<sub>2</sub> initiator shares many features with the Sn(IV) systems discussed in this paper. The general reaction mechanism outlined in Figures 2 and 3 is parallel for the Sn(II) and Sn(IV) systems. It is also found that DXO reacts somewhat faster than LL-lactide with SnOct<sub>2</sub>. This trend has been noted above for DXO and glycolide in tin systems A–D. Also, the highest point on the potential energy surfaces is the transition state equivalent to **TS1** in the case of DXO/SnOct<sub>2</sub> and **TS2** in the case of LL-lactide/SnOct<sub>2</sub>.

The SnOct<sub>2</sub> initiator does have some unique features making it distinct from SnMe<sub>3</sub>MeO and SnMe<sub>2</sub>(MeO)<sub>2</sub>. Our previous work has shown that the bidentate Oct ligands of SnOct<sub>2</sub> can change character during the ROP



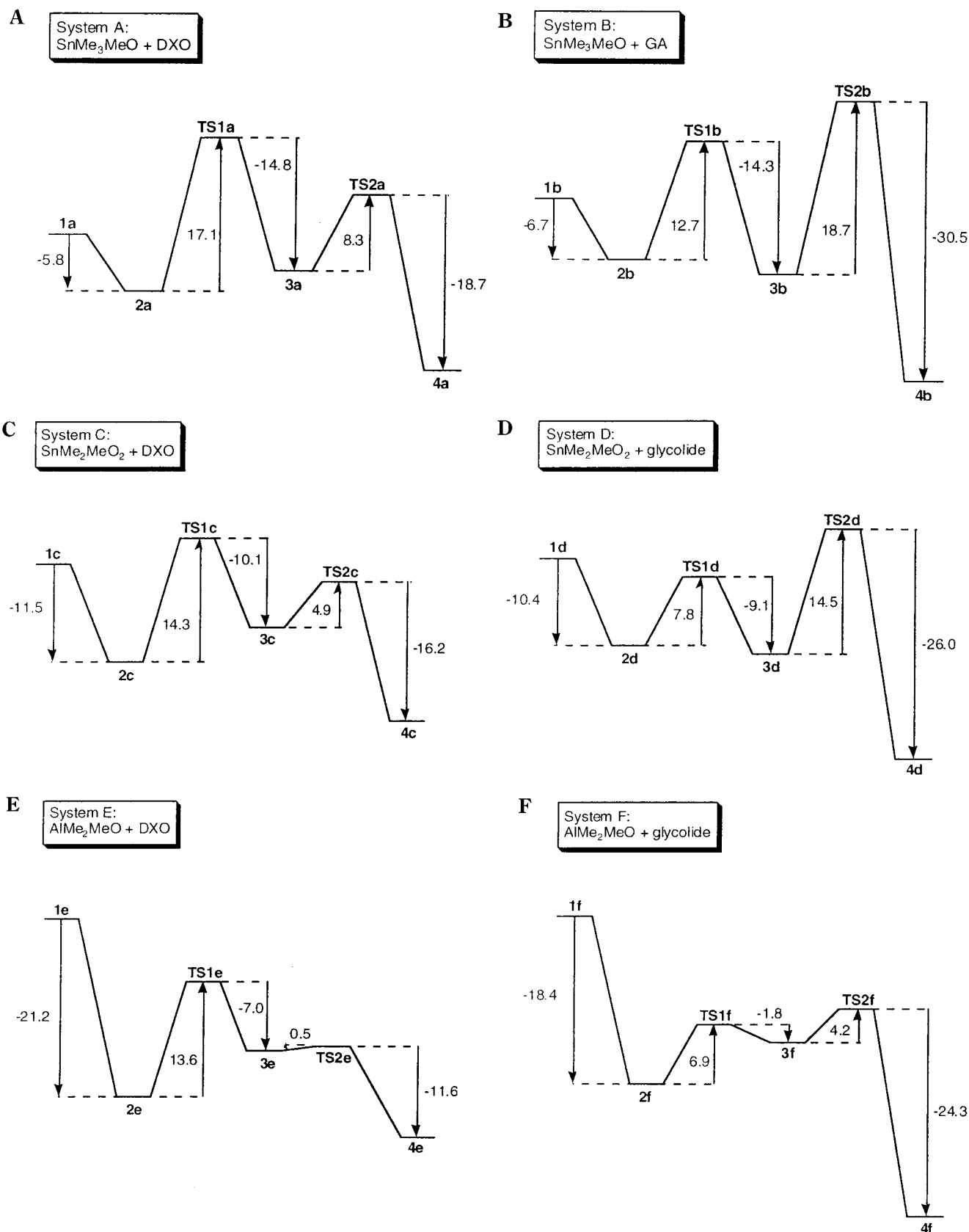


**Figure 4.** Potential energy surfaces for the ROP systems SnMe<sub>3</sub>MeO/DXO (A), SnMe<sub>3</sub>MeO/glycolide (B), SnMe<sub>2</sub>(MeO)<sub>2</sub>/DXO (C), SnMe<sub>2</sub>(MeO)<sub>2</sub>/glycolide (D), AlMe<sub>2</sub>MeO/DXO (E), and AlMe<sub>2</sub>MeO/glycolide (F). Energies are given in kcal/mol.

sequence, fluctuating between states of Oct and OctH character.<sup>11</sup> Furthermore, it has been proposed that the SnOct<sub>2</sub> initiator loses octanoic acid (OctH) prior to the ROP of cyclic esters.<sup>12,53</sup> It was therefore interesting to

see how the electron-accepting ability of possible Sn(II) initiating species correlated to the reactivity.

We have found that the reaction barriers for the ROP of DXO with SnOct'<sub>2</sub>(MeOH)<sub>2</sub>, SnOct'(MeO)MeOH, and

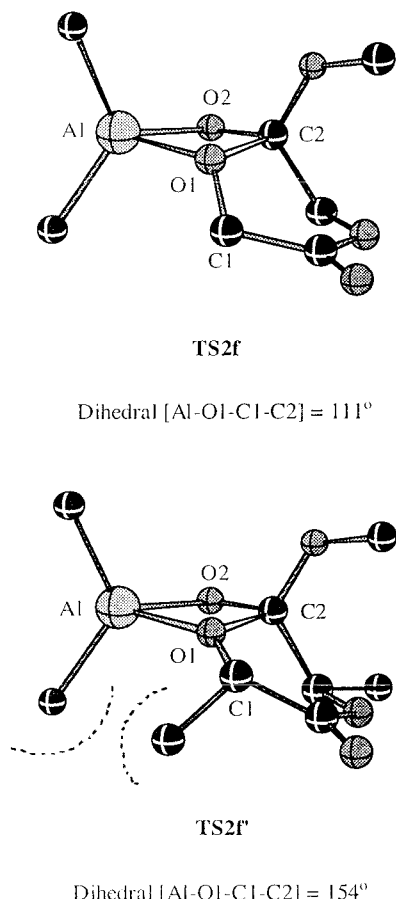


**Figure 5.** Structures of **TS2f** and **TS2f'** showing how steric interactions between methyl groups on the monomer ring and initiator lead to induced strain in the transition state. Hydrogen atoms have been omitted for clarity.

$\text{Sn}(\text{MeO})_2$  to be 19.8, 16.1, and 12.6 kcal/mol, respectively.<sup>11</sup> The second and third of these initiating systems represent situations where one and two acids ( $\text{Oct}'\text{H}$ ) have dissociated. The energy of the LUMO was 5.8 kcal/mol higher for  $\text{SnOct}'_2(\text{MeOH})_2$  compared to  $\text{SnOct}'(\text{MeO})\text{MeOH}$ , which in turn was 29.4 kcal/mol higher than  $\text{Sn}(\text{MeO})_2$ .<sup>54</sup>  $\text{Sn}(\text{MeO})_2$  has a notably more stable LUMO than the other initiating systems and also displays the lowest reaction barrier. As was the case in the  $\text{Sn}(\text{IV})$  and  $\text{Al}(\text{III})$  systems, the overall driving force of the reaction increases with the stability of the initiator. For the ROP of DXO the total exothermicity of the reaction was 11.8 kcal/mol for  $\text{SnOct}'_2(\text{MeOH})_2$ , 12.2 kcal/mol for  $\text{SnOct}'(\text{MeO})\text{MeOH}$ , and 14.3 kcal/mol for  $\text{Sn}(\text{MeO})_2$ . It should be mentioned that the character of the LUMO is notably different for the different tin systems. Experimental work using  $\text{SnOct}_2$  initiators as well as mixtures of  $\text{Sn}(\text{O}i\text{Bu})_2$  and  $\text{OctH}$ <sup>15,47,53,55</sup> confirms this trend in reactivity of  $\text{Sn}(\text{II})$  systems. Duda et al.<sup>53</sup> found that polymerization with  $\text{Sn}(\text{O}i\text{Bu})_2$  was approximately 10 000 times faster than polymerization with  $\text{Sn}(\text{Oct})_2$ .

## Conclusions

We have investigated the ROP of DXO and glycolide with three different initiators:  $\text{SnMe}_3\text{MeO}$ ,  $\text{SnMe}_2(\text{MeO})_2$ , and  $\text{AlMe}_2\text{MeO}$ . It was found that the highest point on the potential energy surface was different for the two monomers. For all three initiators it was found that the transition state involving the breaking of the

carbonyl double bond (**TS1**) represented the least stable structure for DXO. For glycolide, however, it was the transition state structure of the acyl–oxygen cleavage (**TS2**). The reaction barrier varied with both the electronic and steric properties of the monomer.

Comparing the three different initiators, it was found that the stability of the initiator LUMO had a key influence on the reactivity. Both transition states in the proposed reaction sequences (A–F) were lowered with increasing stability of the initiator LUMO. Explicitly, the LUMO energy of the initiators decreased as follows,  $\text{SnMe}_3\text{MeO} > \text{SnMe}_2(\text{MeO})_2 > \text{AlMe}_2\text{MeO}$ , and the reaction barrier followed the same trend for the ROP of both DXO and glycolide. Results also indicate that the reactivity of the more electrophilic aluminum initiators is more sensitive to steric interference.

**Acknowledgment.** The Swedish Research Council for Engineering Sciences, TFR (Grant 210-1999-658), and the Swedish Natural Science Research Council, NFR, are thanked for financial support. H.v.S. thanks the Ernst Johnson foundation for a scholarship. We gratefully acknowledge the Paralleldatorcentrum at the Royal Institute of Technology for providing the computer facilities.

## References and Notes

- (1) Kricheldorf, H. R.; Boettcher, C.; Tonnes, K. U. *Polymer* **1992**, *33*, 2817–2824.
- (2) Kricheldorf, H. R.; Lee, S. R. *Macromolecules* **1995**, *28*, 6718–6725.
- (3) Kricheldorf, H. R.; Lee, S. R. *Macromol. Chem. Phys.* **1994**, *195*, 2299–2306.
- (4) Spassky, N.; Wisniewski, M.; Pluta, C.; LeBorgne, A. *Macromol. Chem. Phys.* **1996**, *197*, 2627–2637.
- (5) Jacobs, C.; Dubois, P.; Jerome, R.; Teyssie, P. *Macromolecules* **1991**, *24*, 3027–3034.
- (6) Stridsberg, K.; Albertsson, A.-C. *J. Polym. Sci., Part A: Polym. Chem.* **1999**, *37*, 3407–3417.
- (7) Stridsberg, K.; Ryner, M.; Albertsson, A.-C. *Macromolecules* **2000**, *33*, 2862–2869.
- (8) Dubois, P.; Jacobs, C.; Jerome, R.; Teyssie, P. *Macromolecules* **1991**, *24*, 2266–2270.
- (9) Lofgren, A.; Albertsson, A.-C. *Polymer* **1995**, *36*, 3753–3759.
- (10) Duda, A.; Florjanczyk, Z.; Hofman, A.; Slomkowski, S.; Penczek, S. *Macromolecules* **1990**, *23*, 1640–1646.
- (11) Ryner, M.; Stridsberg, K.; Albertsson, A. C.; von Schenck, H.; Svensson, M. *Macromolecules* **2001**, *34*, 3877–3881.
- (12) Kowalski, A.; Duda, A.; Penczek, S. *Macromolecules* **2000**, *33*, 7359–7370.
- (13) Kowalski, A.; Duda, A.; Penczek, S. *Macromolecules* **2000**, *33*, 689–695.
- (14) Kowalski, A.; Duda, A.; Penczek, S. *Macromol. Rapid Commun.* **1998**, *19*, 567–572.
- (15) Kricheldorf, H. R.; Kreiser-Saunders, I.; Stricker, A. *Macromolecules* **2000**, *33*, 702–709.
- (16) Penczek, S.; Duda, A.; Libiszowski, J. *Macromol. Symp.* **1998**, *128*, 241–254.
- (17) Ropson, N.; Dubois, P.; Jerome, R.; Teyssie, P. *Macromolecules* **1995**, *28*, 7589–7598.
- (18) Lofgren, A.; Albertsson, A.-C.; Dubois, P.; Jerome, R.; Teyssie, P. *Macromolecules* **1994**, *27*, 5556–5562.
- (19) Eguiburu, J. L.; Fernandez-Berridi, M. J.; Cossio, F. P.; San Roman, J. *Macromolecules* **1999**, *32*, 8252–8258.
- (20) Stridsberg, K.; Albertsson, A.-C. *J. Polym. Sci., Part A: Polym. Chem.* **2000**, *38*, 1774–1784.
- (21) Kricheldorf, H. R.; Langanke, D.; Spickermann, J.; Schmidt, M. *Macromolecules* **1999**, *32*, 3559–3564.
- (22) Kricheldorf, H. R.; Langanke, D. *Macromol. Chem. Phys.* **1999**, *200*, 1183–1190.
- (23) Kricheldorf, H. R.; Stricker, A.; Langanke, D. *Macromol. Chem. Phys.*, in press.
- (24) Kricheldorf, H. R.; Lee, S. R. *Macromolecules* **1996**, *29*, 8689–8695.
- (25) Musaev, D. G.; Morokuma, K. *J. Phys. Chem.* **1996**, *100*, 6509–6517.

- (26) Stevens, P. J.; Devlin, F. J.; Chabrowski, C. F.; Frisch, M. J. *J. Phys. Chem.* **1994**, *98*, 11683–11687.
- (27) Erikson, L. A.; Pettersson, L. G. M.; Siegbahn, P. E. M.; Wahlgren, U. *J. Chem. Phys.* **1995**, *102*, 872–878.
- (28) Ricca, A.; Bauschlicher, J.; C. W. *J. Phys. Chem.* **1994**, *98*, 12899–12903.
- (29) Heinemann, C.; Hertwig, R. H.; Wesendrup, R.; Koch, W.; Schwarz, H. *J. Am. Chem. Soc.* **1995**, *117*, 495–500.
- (30) Hertwig, R. H.; Hrusak, J.; Schröder, D.; Koch, W.; Schwarz, H. *Chem. Phys. Lett.* **1995**, *236*, 194–200.
- (31) Schröder, D.; Hrusak, J.; Hertwig, R. H.; Koch, W.; Schwerdtfeger, P.; Schwarz, H. *Organometallics* **1995**, *14*, 312–316.
- (32) Fiedler, A.; Schröder, D.; Shaik, S.; Schwarz, H. *J. Am. Chem. Soc.* **1994**, *116*, 10734–10741.
- (33) Fan, L.; Ziegler, T. *J. Chem. Phys.* **1991**, *95*, 7401–7408.
- (34) Berces, A.; Ziegler, T.; Fan, L. *J. Phys. Chem.* **1994**, *98*, 1584–1595.
- (35) Lyne, P. D.; Mingos, D. M. P.; Ziegler, T.; Downs, A. J. *Inorg. Chem.* **1993**, *32*, 4785–4796.
- (36) Li, J.; Schreckenbach, G.; Ziegler, T. *J. Am. Chem. Soc.* **1995**, *117*, 486–494.
- (37) Gaussian 98, Revision A.3: Frisch, M. J.; Trucks, G. W.; Schlegel, H. B.; Scuseria, G. E.; Robb, M. A.; Cheeseman, J. R.; Zakrzewski, V. G.; Montgomery, J. A., Jr.; Stratmann, R. E.; Burant, J. C.; Dapprich, S.; Millam, J. M.; Daniels, A. D.; Kudin, K. N.; Strain, M. C.; Farkas, O.; Tomasi, J.; Barone, V.; Cossi, M.; Cammi, R.; Mennucci, B.; Pomelli, C.; Adamo, C.; Clifford, S.; Ochterski, J.; Petersson, G. A.; Ayala, P. Y.; Cui, Q.; Morokuma, K.; Malick, D. K.; Rabuck, A. D.; Raghavachari, K.; Foresman, J. B.; Cioslowski, J.; Ortiz, J. V.; Stefanov, B. B.; Liu, G.; Liashenko, A.; Piskorz, P.; Komaromi, I.; Gomperts, R.; Martin, R. L.; Fox, D. J.; Keith, T.; Al-Laham, M. A.; Peng, C. Y.; Nanayakkara, A.; Gonzalez, C.; Challacombe, M.; Gill, P. M. W.; Johnson, B.; Chen, W.; Wong, M. W.; Andres, J. L.; Gonzalez, C.; Head-Gordon, M.; Replogle, E. S.; Pople, J. A. Gaussian, Inc., Pittsburgh, PA, 1998.
- (38) Hay, P. J.; Wadt, W. R. *J. Chem. Phys.* **1985**, *82*, 299–310.
- (39) Wadt, W. R.; Hay, P. J. *J. Chem. Phys.* **1985**, *82*, 284–289.
- (40) Dunning, T. M., Jr. *J. Chem. Phys.* **1970**, *53*, 2823–2833.
- (41) Dunning, T. M., Jr. *J. Chem. Phys.* **1971**, *55*, 716–723.
- (42) McLean, A. D.; Chandler, G. S. *J. Chem. Phys.* **1980**, *72*, 5639–5648.
- (43) Krishnan, R.; Binkley, R. S.; Seeger, R.; Pople, J. A. *J. Chem. Phys.* **1980**, *72*, 650–654.
- (44) One C–O bond was broken homolytically, and the new energies for DXO and glycolide were calculated to 96.4 and 92.2 kcal/mol, respectively.
- (45) Ryner, M.; Finne, A.; Albertsson, A.-C.; Kricheldorf, H. R. *Macromolecules* **2001**, *34*, 7281–7287.
- (46) Baran, J.; Duda, A.; Kowalski, A.; Szymanski, R.; Penczek, S. *Macromol. Symp.* **1997**, *123*, 93–101.
- (47) Kowalski, A.; Libiszowski, J.; Duda, A.; Penczek, S. *Macromolecules* **2000**, *33*, 1964–1971.
- (48) Dubois, P.; Ropson, N.; Jerome, R.; Teyssie, P. *Macromolecules* **1996**, *29*, 1965–1975.
- (49) Löfgren, A.; Albertsson, A.-C., unpublished results.
- (50) The difference between structures **2f'** and **TS2f'** was 13.1 kcal/mol.
- (51) The difference between structures **2b'** and **TS2b'** was 19.3 kcal/mol.
- (52) The absolute values of the SnMe<sub>3</sub>MeO, SnMe<sub>2</sub>(MeO)<sub>2</sub>, and AlMe<sub>2</sub>MeO LUMOs are 0.331, 0.049, and –0.127 eV, respectively.
- (53) Duda, A.; Penczek, S.; Kowalski, A.; Libiszowski, J. *Macromol. Symp.* **2000**, *153*, 41–53.
- (54) The absolute values of the SnOct'<sub>2</sub>(MeOH)<sub>2</sub>, SnOct'(MeO)-MeOH, and Sn(MeO)<sub>2</sub> LUMOs are –0.373, –0.626, and –1.648 eV, respectively.
- (55) Kricheldorf, H. R.; Kreisersaunders, I.; Boettcher, C. *Polymer* **1995**, *36*, 1253–1259.

MA011653I